
Fracture Toughness of Heavy Section Ductile Iron Castings and Safety Assessment of Cast Casks

N. Urabe¹ and Y. Harada²

¹*NKK Corporation, Kawasaki-city*

²*NKK Corporation, Yokohama-city, Japan*

INTRODUCTION

The strategy for interim storage of nuclear spent fuel prior to reprocessing is established in Japan. We propose to develop technical schemes for dry metal cask storage, i.e., to prove the practicality of ductile cast iron casks. To successfully meet this goal, the Central Research Institute of Electric Power Industry has organized a QA Committee to address the technical issues regarding the quality assurance of DCI casks. The CRIEPI plans to confirm the adequacy of this spent fuel storage technology through round robin material tests by the committee and verification testing programs under the sponsorship of the Ministry of International Trade and Industry. Participating in the CRIEPI's programs, the NKK Corporation is now struggling with the development of reliable and high performable DCI casks.

This paper summarizes the results of a series of studies performed to determine the fracture toughness of heavy section ductile iron castings and the safety of DCI casks based on the results of the probabilistic fracture mechanics analysis and the quality assurance method for production casks.

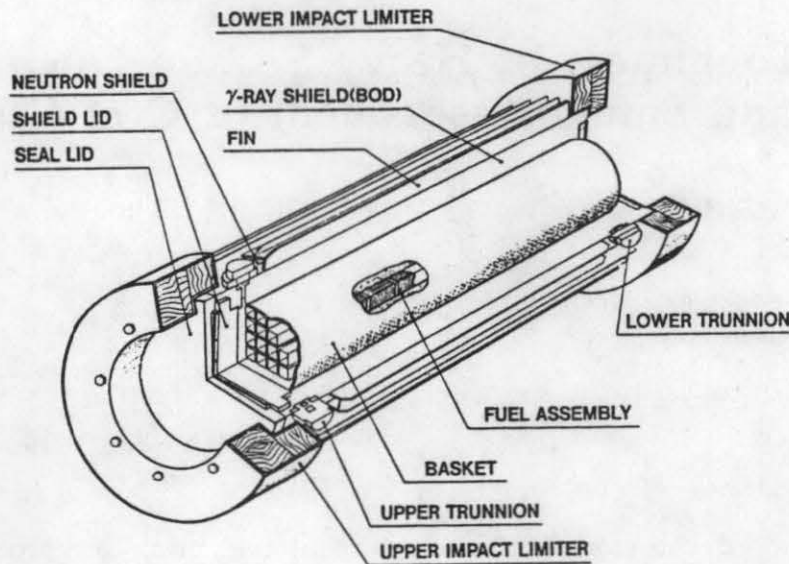
OUTLINE OF NK-DTS CASK

A schematic drawing of NK-DTS (Dry Transportation and Storage) cask is shown in Fig. 1. The nuclear spent fuel assembly is separately put in a borated stainless

Namio Urabe¹ and Yoshihiko Harada²

¹*Steel Research Center, NKK Corporation, Kawasaki-city, Japan*

²*Nuclear Plant Department, NKK Corporation, Yokohama-city, Japan*



Type	Max. Weight (ton f)	Number of SF	Length (m)	Out side dia. (m)
BWR Type	107	52	5480	2140
	82	32	5350	1740
PWR Type	112	21	5030	2200
	84	12	4980	1890

Fig.1 NKK dry transportation/storage cask

steel basket inside the cask to keep the fuel being sub-critical. The gamma-ray is shielded completely by the cask body (production of ductile cast iron) and by the duplex lids of stainless steel. The decay heat is radiated out by the fins fixed on the outside surface of the body and the neutron is again shielded by the material (i.e., epoxy or polyethylene) put between the radiation fins. A pair of impact limiters are installed on the top and the bottom end of the cask in order to absorb the impact load due to accident.

To produce the cask body, a Hot Direct Casting Method has been adopted. It is a continuous process from the hot metal tapping at the blast furnace to the casting without intermediate solidification. The process is shown in Fig. 2. The hot metal is firstly desiliconized and desulfurized, then a New Refining Process (Yamase et al. 1987) is applied to reduce the phosphorus level and to adjust the carbon and silicon contents. Immediately after those processes spheroidization and inoculation treatments are completed and the casting process is followed. According to the casting design based on the results of solidification analysis, and the standards for hot metal temperature, casting temperature and quality assurance, a high performable and reliable ductile cast iron cask body is

manufactured. After being checked the quality, the casting is sent to the machine factory to assemble the radiation fins, the neutron shielding material, the borated stainless steel basket and the impact limiters. Thus, the NK-DTS cask is accomplished.

FRACTURE TOUGHNESS OF HEAVY SECTION DUCTILE CAST IRON

Model Casks and Extraction of Specimens

The model casks made by ductile cast iron: model cask S (outer diameter=2222 mm, wall thickness=360mm, length=3000mm) and model cask H(od=2300mm, t=400mm, ℓ=2130mm) were used to examine the distribution of fracture toughness, other mechanical properties, physical and metallurgical properties throughout the cask body. Both models are scaled down only the length from the NK-DTS cask. Several blocks were cut out from the top, middle, bottom, corner

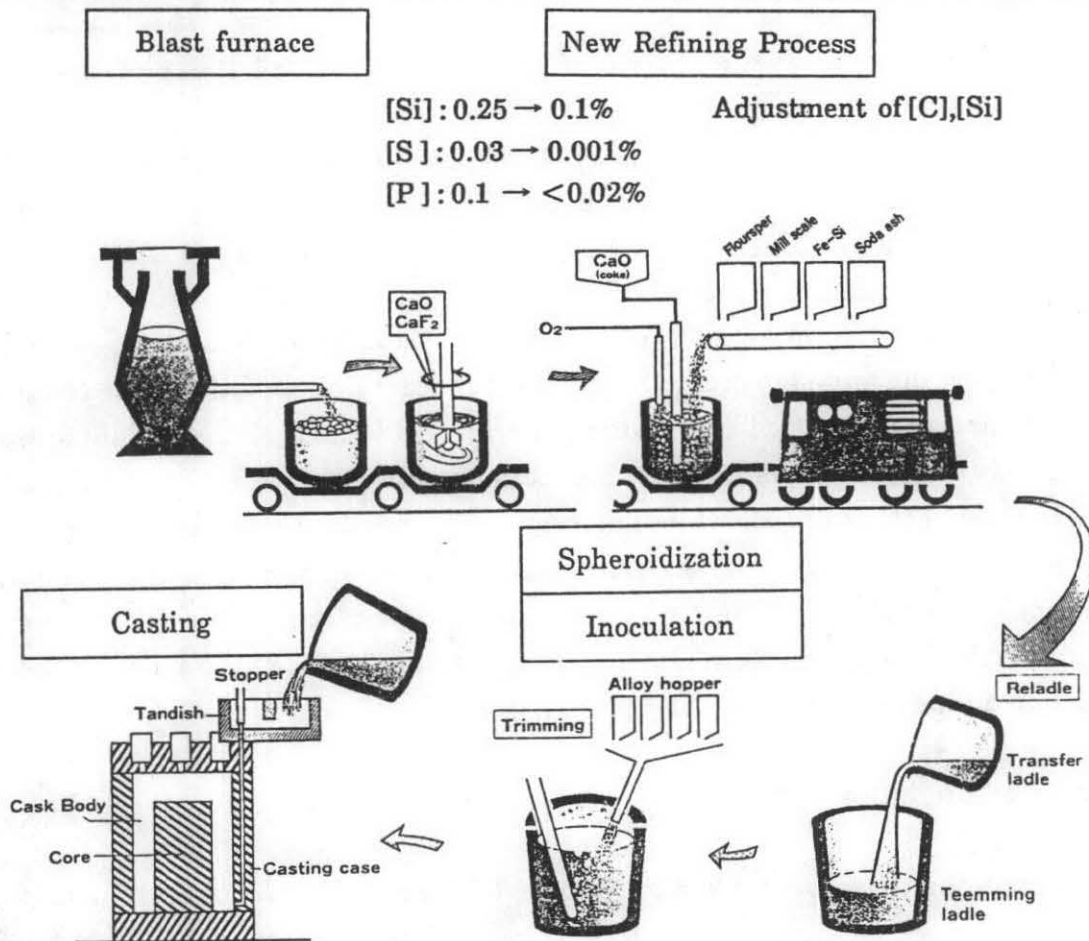


Fig. 2 Hot direct casting process for NKK cask

and sole portion, then various test pieces were machined from each block. The cutting scheme is shown in Fig. 3. According to the preliminary test results made

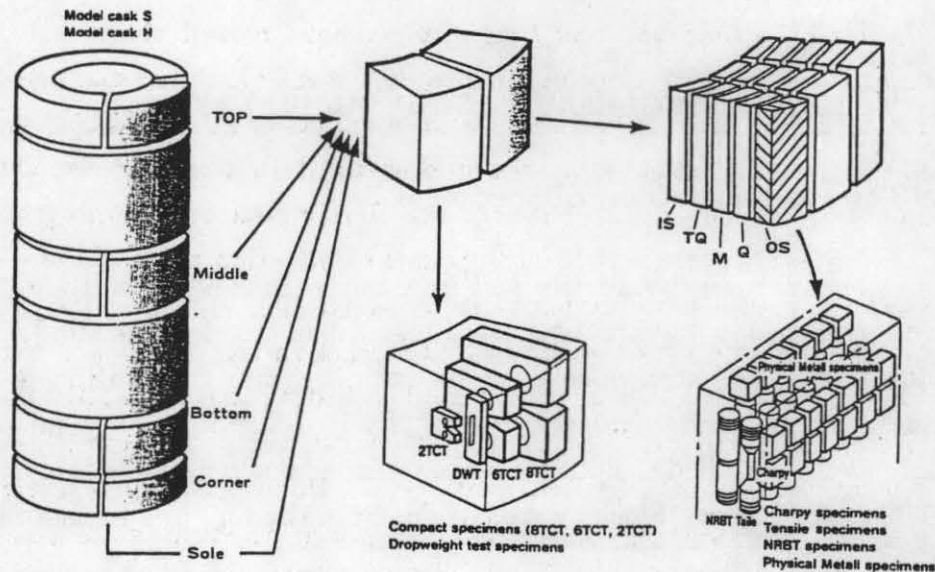


Fig. 3 A cutting scheme of specimens from model casks

for the specimen thickness dependence of fracture toughness and the applicability of linear elastic fracture mechanics to the ductile cast iron (Saegusa and Urabe 1989), 6TCT(150mm thick) and 8TCT (200mm thick) specimens (ASTM 1983) were selected to measure the critical stress intensity factor K_{IC} . In a few 6TCT specimens, side-face-grooves (15mm deep, 45° flank angle, 0.25mm groove tip radius) were machined in order to increase the constraint condition. The compact specimens were extracted so that the pre-crack tip located at the middle of wall thickness, since here has the weakest toughness due to the slowest cooling rate during the casting process (this has been confirmed by the fracture toughness tests using small size specimen). The tensile, Charpy impact, notched round bar in tension (NRBT), drop weight test specimens and specimens for physical and metallurgical properties were also extracted from the blocks at the each thickness location divided into five sections (see Fig.3).

Fracture Toughness Tests

Fracture toughness tests by 8TCT and 6TCT and also 2TCT (50mm thick) specimens were performed in conformity with the test method of ASTM-E399 (ASTM 1983). Before the tests, fatigue pre-crack was introduced at ambient temperature with maximum stress intensity factor range between 75 and

90kgf/mm^{3/2}. The test temperature was between 0 and -100°C and the stress intensity factor rate was between 10 and 10⁴kgf/mm^{3/2}s.

For the case of the load vs. load line displacement record showed an elastic manner until the brittle failure occurrence, K_Q was calculated and the K_Q was recognized as $K_{IC,R}$ if it satisfied the requirements of the ASTM-E399 standard. Otherwise, or a plastic behaviour was dominant in the load vs. load line displacement record, the absorbed energy was firstly obtained by integrating the load vs. load line displacement record up to the deflection point of the electrical potential vs. load line displacement curve recorded simultaneously. The deflection point corresponds to the ductile crack initiation prior to the brittle failure. Then, J-integral, J_i was determined according to ASTM-E813 standards (ASTM 1987). If the J_i satisfied the requirements, the J_i was converted to the stress intensity factor and described as $K_{IC,R}^{J_i}$. In this report, the loading rate of all the fracture toughness test exceeded 8.8kgf/mm^{3/2} s that is the upper limit for the static test condition. Therefore, the suffix R was attached to the K_{IC} to denote the rapid load fracture toughness described in the Annex 7 in ASTM-E399.

For the quality assurance of the production cask, small size NRBT specimens with fatigue pre-crack were adopted. The configuration and dimensions are shown in Fig. 4. The \dot{K}_I and the J for the NRBT specimen are given by eqs. (1)

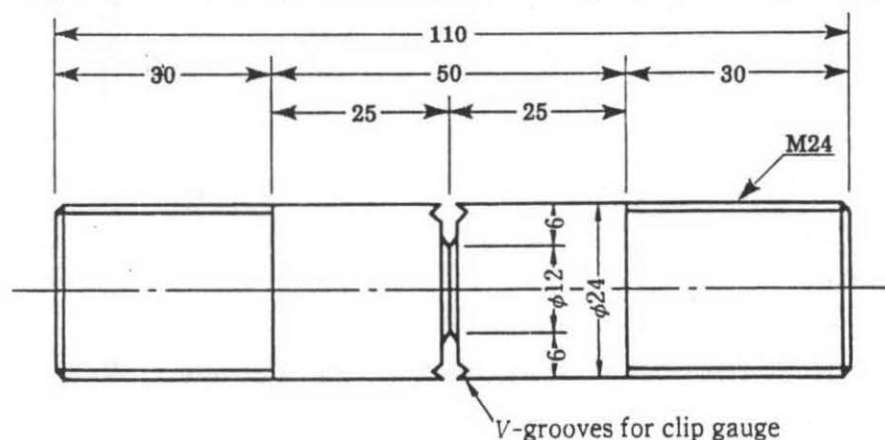


Fig. 4 Dimensions of NRBT specimen

and (2), respectively (Benthem and Koiter 1973, Rice et al. 1973).

$$K = \frac{P}{nb^2} \sqrt{nb} \left[\frac{1}{2} \left\{ 1 + \frac{b}{2R} + \frac{3}{8} \left(\frac{b}{R} \right)^2 - 0.363 \left(\frac{b}{R} \right)^3 + 0.731 \left(\frac{b}{R} \right)^4 \right\} \right] \sqrt{1 - \frac{b}{R}} \quad (1)$$

$$J = \frac{1}{2nb^2} \left[3 \int_0^V PdV - PV \right] \quad (2)$$

where, P is the load, b is the ligament radius, R is the radius of specimen and V is the crack mouth opening displacement. The validity requirement for the NRBT specimens and the side-face-grooved 6TCT specimens, eq.(3) was derived, since the plane strain condition is satisfied along the whole length of the pre-crack front.

$$(B,a)_{\min} \geq 0.83(K_Q/\sigma_y)^2 \quad (3)$$

where, B is the specimen thickness or the radius (b), a is the pre-crack length and σ_y is the yield strength. The temperature and strain rate dependence of yield strength is estimated by eq. (4) that is best fit equation for the experimental results.

$$\sigma_y(T, \dot{\epsilon}) = \sigma_{y0} - 4.58 + 3600/T + 1.96 \log \dot{\epsilon} \quad (4)$$

And the relationship between stress intensity factor rate \dot{K}_I and strain rate $\dot{\epsilon}$ is also derived as eq. (5) (Urabe et al. 1984)

$$\dot{\epsilon} = \frac{K_{IC} \dot{K}_I}{1.8 \rho \sigma_y E} \quad (5)$$

In eqs. (4) and (5), σ_{y0} is the yield strength at ambient temperature and $\dot{\epsilon}$ being $10^{-4}/s$, T is the absolute temperature, E is Young's modulus and $\rho\sigma$ is taken as 0.03mm.

The drop weight tests were conducted in conformity with ASTM-E208 (ASTM 1987). The specimen size was P-3 (16mm thick, 50mm wide, 130mm long) and the drop weight energy was 34kgfm.

Lower Bound Fracture Toughness

The results of statistical analysis made on the fracture toughness is shown in Table 1. The samples are classified by the same test condition. Every sample fits well to the two parameter Weibull distribution function. Using the samples 2 - 5, curves for the accumulated fracture probability being 50, 1 and 0.1% are obtained as a function of the temperature $T-T_{NDT}$. The reference fracture toughness curve for ASTM SA533 Gr.B and SA508 steels described in ASME Boiler and Pressure Vessel Code (ASME 1983) is also taken into consideration. The fracture toughness of heavy section ductile cast iron with the failure probability of 0.1% is situated above the ASME's curve.

Sample	T (°C)	\dot{K}_I (kg/mm ^{3/2} s)	TP size x No. of TP	Shape parameter α	Scale parameter β	Expected value μ (kg/mm ^{3/2})	Stand. deviation σ (kg/mm ^{3/2})	Remarks
1	-40	10 ³	6TCT x 9	14.55	249.17	240.35	20.85	7 model casks (QA comm.)
2	-40	10 ³ /10 ⁴	6TCT x 12	10.88	246.30	235.02	26.76	Model cask S
3	-100	10	2TCT x 22	14.10	142.30	137.21	11.91	Model cask S
4	-40	10 ³ /10 ⁴	6TCT, 8TCT x 9	14.46	359.74	347.01	29.33	Model cask H
5	-70	10 ³ /10 ⁴	6TCT, 8TCT x H	11.93	279.81	268.06	27.32	Model cask H

Table 1 Result of statistical analysis of fracture toughness

Now assuming eq.(6) is the lower bound fracture toughness curve for the DCI, every data which we have obtained, including the results of the round robin tests of the QA committee (CRIEPI, 1988) are plotted in Fig. 5 as a function of temperature.

$$K_{IC,R} = 95 + 4.3 \exp[0.026(T + 160)] \quad (6)$$

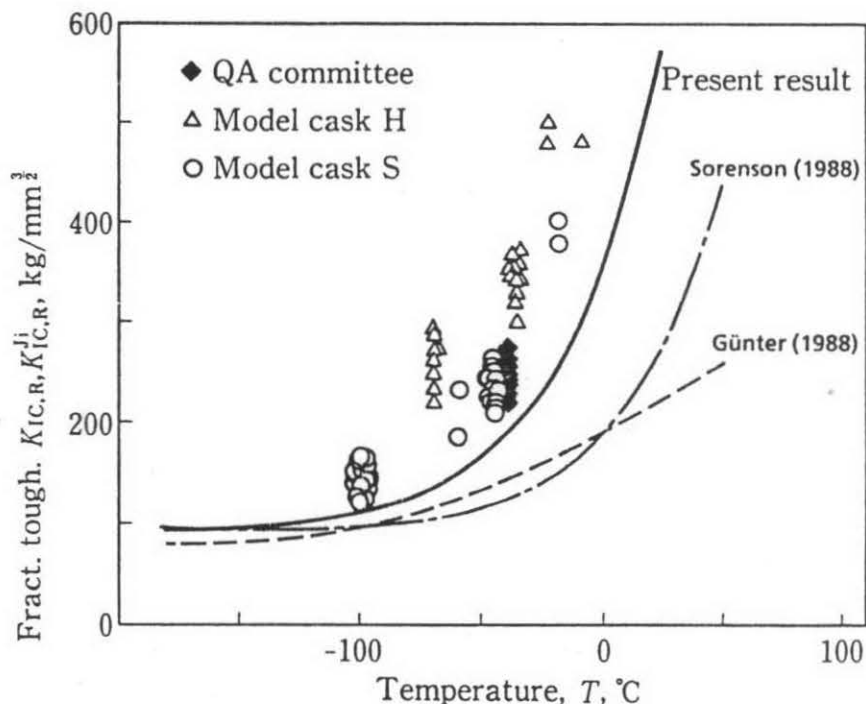


Fig. 5 Proposed reference fracture toughness of heavy section ductile cast iron

where $K_{IC,R}$ is the rapid load fracture toughness and T is the temperature ($^{\circ}\text{C}$). No data exists below the lower bound curve. The other lower bound curves are also drawn in Fig. 5. The dotted curve is the proposal by the Federal Republic of Germany for DIN-GGG40 (Günter 1988) and the chained one is that by the United States for ASTM-A874 where the T_{NDT} is assumed to be -29°C (Sorenson

1988). The curve by eq. (6) seems unconservative for the warrant value if it is compared with the other proposals, but it is conservative if eq. (6) is read as the requisite fracture toughness of DCI, Thus, eq. (6) could be a candidate for the reference fracture toughness curve of the DCI for cast cask, if the value is proved to exceed the requirement which will be established.

SAFETY ANALYSIS

Safety Analysis against Brittle Failure

Assuming a cast cask weighing 125 tonf, cooled down to -40°C , with semi-elliptic surface crack (a mm deep, $2c$ mm long, $2c/a = 6$) at the maximum stressed location under the 9-meter drop test of horizontal position, the failure probability of brittle fracture was calculated. The result is shown in Fig. 6. The P_f increases from 10^{-8} to 10^{-5} if the crack depth increases from 30mm to 70mm.

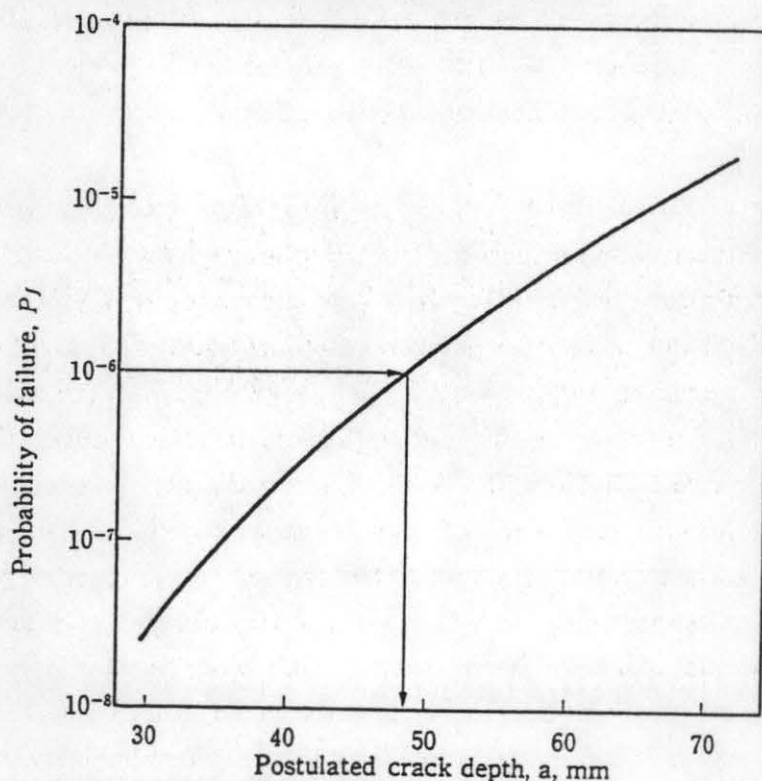


Fig. 6 Failure probability vs. postulated crack size

We do not know yet the suitable failure probability level for the safety of the cast cask. But the failure probability of 10^{-6} is defined by the NRC as "extremely low in the case of the primary coolant loop pipe rupture for the PWR" (NRC 1987) and

it is reported that "we do not need to consider any effective actions for the component failure in the atomic energy industry if the probability is less than 10^{-6} " (RSK 1981). Moreover, in the aircraft industry, the defect detectability rule for NDE is determined on the basis that the failure probability should be less than 10^{-6} even though the crack is overlooked by the investigation (Benoy, 1981). Adopting the above concept for the 9-meter drop test, the defect size causes the failure probability of 10^{-6} is read as 49mm from Fig. 6.

Now let the requisition value of the stress intensity factor be that of the maximum impact stress of 8.1kgf/mm^2 exerted on the surface crack of 49mm deep and 294mm long. The $K_{I,REQ}$ is $99\text{kgf/mm}^{3/2}$. On the other hand, the reference fracture toughness $K_{IC,R}$ at -40°C by eq (6) is $192\text{kgf/mm}^{3/2}$. The $K_{IC,R}$ exceeds enough the requirement. The proposed values by the USA and the FRG also satisfy this requirement. Taking the first moment of the distributions the averages of $K_{IC,R}$ and K_I are obtained as $\mu_{FT} = 235.0\text{kgf/mm}^{3/2}$ and $\mu_K = 89.3\text{kgf/mm}^{3/2}$, respectively. If the safety factor is defined as the ratio of μ_{FT} and μ_K , the safety margin is 2.6 for the above analysis.

Moreover, the crack size of 49mm is the allowable crack size. Even if the crack of 49mm exists in the cask body, the DCI cask of average fracture toughness being more than $235\text{kgf/mm}^{3/2}$ never fails when it is encountered with the postulated accident equivalent to the 9-meter drop test. Thus, we must assure by the NDE that no defect larger than 49mm exists in the cask body. Let the safety factor be also 2.6 for the NDE as same as the failure probability, the detectability limit of NDE is obtained as $a_{NDE} = 49/(2.6)^2 = 7.3\text{mm}$, since the stress intensity factor is proportional to the square root of the crack size. Namely, we need a nondestructive test method to detect a surface crack or an embedded crack size of 7.3mm or 14.6mm, respectively with the detectability of 100%. By the ultrasonic investigation conducted on the heavy section DCI blocks it has been concluded that the crack size of 100% detectability was as small as 5mm. The same ultrasonic test was performed on the model casks, and it has been reported that no defect exists. Meanwhile, no visible defect was detected when the visual check was made on the surfaces of the blocks, the test pieces and the fractured surfaces. This implies that the reliability of the NDE with the accuracy of 5mm is quite reasonable.

CONCLUSIONS

In order to make safety assessment of the DCI casks against the brittle failure, the fracture toughness of heavy section ductile cast iron was thoroughly investigated. Using the results, the safety assessment of DCI casks was performed based on the probabilistic fracture mechanics. The NK - DTS cask is proved as safety enough even if it is encountered with the accident during the transportation or the management at the storage facilities. A quality assurance method for the production casks is also proposed.

REFERENCES

- ASME, Boiler and Pressure Vessel Code, Sect. III, "Rules for Construction of Nuclear Power Plant Component" Appendix G, "Protection against Nonductile Failure" (1983)
- ASTM, "Standard Test Method for Plane-Strain Fracture Toughness of Metallic Materials" E-399 (1983)
- ASTM, "Standard Method for Conducting Drop-Weight Test to Determine Nil-Ductility Transition Temperature of Ferritic Steels" E-208 (1987)
- ASTM, "Standard Test Method for J_{IC} , A Measure of Fracture Toughness" E-813 (1987)
- Benoy, M.B. "Fatigue Life Variability in Civil Aircraft" Proc. 11th ICAF Symposium (1981)
- Benthem, J.P. and Koiter, W.T., "Asymptotic Approximations to Crack Problems. Method of Analysis and Solutions of Crack Problems" Noodhoff Inc. Pub. (1973) p.131
- CENTRAL RESEARCH INSTITUTE, "Research on Quality Assurance of Ductile Cast Iron casks", CRIEPI Report, April (1988)
- Günter, B. "DCI Cask Technology in FRG" Proc. of Int. Symp. on Spent Fuel Storage. Tokyo (1988)
- NRC, "Modification of General Design Criterion" 4, Requirements for Protection Against Dynamic effects of Postulated Pipe Rupture" 10CFR50 (1983)
- Rice, J.R., et al., "Some Further Results of J-Integral Analysis and Estimates" ASTM STP536 (1973) p.231
- Reaktor-Sicherheitskommission, Protokoll der 164, (1981)
- Saegusa, T. and Urabe, N., "Applicability of Linear Elastic Fracture Mechanics to DCI" to be published in J. Atomic Energy Society of Japan (1989)
- Sorenson, K.B., "DCI Cask Research in USA" Proc. of Int. Symp. on Spent Fuel Storage. Tokyo (1988)
- Urabe, N. et al., "Safety Assessment of Steels and Welds Under Cyclic and Monotonic Loadings at Low Temperature" Trans. ASME, Vol.106 (1984) p.473
- Yamase, O., et al., "BOF Technic based on Pre-Treatment Hot Metal" NKK Technical Report, Vol.118 (1987) p.1